NUWC-NPT Technical Report 10,294
16 November 1993

A Microfabricated Surface for Turbulence Control

P. R. Bandyopadhyay
Weapons Technology and Undersea Systems Department

Naval Undersea Warfare Center Division Newport, Rhode Island

Approved for public release; distribution is unlimited.

PREFACE

This report was funded under NUWC Project No. A10301, "Microfabrication," principal investigator P. R. Bandyopadhyay (Code 8233). The sponsoring activity is the Naval Undersea Warfare Center Division Newport Independent Research Program, program manager K. M. Lima (Code 102).

The technical reviewer for this report was R. B. Philips (Code 8233).

The author wishes to thank W. L. Keith (Code 2141) for his assistance with the water tunnel experiments, and also acknowledges the assistance of J. R. Longacre, G. K. Pitcher, R. L. Powell, J. M. Powers, and R. A. Roush with the model fabrication and measurements.

Reviewed and Approved: 16 November 1993

F. L. White
Head, Weapons Technology and Undersea Systems Department

REPORT DOCUMENTATION PAGE

Form Approved
OMB No. 0704-0188

1. AGENCY USE ONLY *(Leave blank)*

2. REPORT DATE
16 November 1993

3. REPORT TYPE AND DATES COVERED

4. TITLE AND SUBTITLE
A Microfabricated Surface for Turbulence Control

5. FUNDING NUMBERS

6. AUTHOR(S)
P. R. Bandyopadhyay

7. PERFORMING ORGANIZATION NAME(S) AND ADDRESS(ES)
Naval Undersea Warfare Center Division
1176 Howell Street
Newport, Rhode Island 02841-1708

8. PERFORMING ORGANIZATION REPORT NUMBER
TR 10,294

9. SPONSORING/MONITORING AGENCY NAME(S) AND ADDRESS(ES)

10. SPONSORING/MONITORING AGENCY REPORT NUMBER

11. SUPPLEMENTARY NOTES

12a. DISTRIBUTION/AVAILABILITY STATEMENT
Approved for public release; distribution is unlimited.

12b. DISTRIBUTION CODE

13. ABSTRACT *(Maximum 200 words)*

Emerging technology of microfabrication is being applied to develop a surface for turbulence quieting and drag reduction of hydrodynamic and aerodynamic vehicles. Because Reynolds number is known to strongly affect the structure and statistics of a turbulent boundary layer, development is aimed at high Reynolds number applications right from the beginning. Very short length and time scales, like a few hundreds of microns and milliseconds, respectively, are associated with high Reynolds number flows. This requirement can only be met by microfabrication technology. Thus, the microfabrication aspect of the development of the surface is a crucial part of this research.

This document presents the preliminary tests that were carried out in a quiet-water tunnel, and the deflection characteristics of the elastic components that were measured. The engineering performance was encouraging, and no adverse hydrodynamic effects were observed.

14. SUBJECT TERMS
Fluid dynamics
Microfabrication

15. NUMBER OF PAGES
20

16. PRICE CODE

17. SECURITY CLASSIFICATION OF REPORT	18. SECURITY CLASSIFICATION OF THIS PAGE	19. SECURITY CLASSIFICATION OF ABSTRACT	20. LIMITATION OF ABSTRACT
UNCLASSIFIED	UNCLASSIFIED	UNCLASSIFIED	SAR

TABLE OF CONTENTS

Section		Page
	LIST OF TABLES	ii
	LIST OF ABBREVIATIONS AND ACRONYMS	ii
1	INTRODUCTION	1
2	OBJECTIVES	3
3	APPROACH AND PROGRESS	5
3.1	Fabrication of Elastic Microfabricated Surfaces (EMFS)	6
3.2	Hydro-Elastic Properties of EMFS Lids	10
3.3	Water Tunnel Tests	11
4	FUTURE WORK	13
5	CONCLUSIONS	15
6	BIBLIOGRAPHY	17

LIST OF ILLUSTRATIONS

Figure		Page
1	Sketch of the Flow Model and Control Concept	2
2	Top View of the Surface	6
3	Sectional Side View of the Area Marked A in Figure 2	7
4	Scanning-Electron-Microscopic View of the Microfabricated Surface Elements	7
5	Dimensions of the Surface-Top After Microfabrication	8
6	Water Tunnel Test Plug Containing the EMFS	8
7	Photograph of the Water Tunnel Test Plug	9
8	Elastic Lid Deflection Characteristics Under a Pressure Differential Loading	10
9	Comparison of Wall-Pressure Spectra ~2.5δ Downstream of the EMFS in the Water Tunnel	11
10	Comparison of Wall-Pressure Spectra 0.54δ Downstream of the EMFS in the Water Tunnel	12
11	Schematic of the Integrated Drag Sensor, EMFS, and Actuator	13

LIST OF TABLES

Table		Page
1	Typical Specifications of the Turbulent Boundary Layer	5

LIST OF ABBREVIATIONS AND ACRONYMS

BTV	Buoyant test vehicle
EMFS	Elastic microfabricated surface
MEMS	Micro-electro-mechanical systems
NLON	Naval Undersea Warfare Center Detachment, New London, CT
SEM	Scanning electron microscope

A MICROFABRICATED SURFACE FOR TURBULENCE CONTROL

1. INTRODUCTION

Recent attempts to control the production of turbulence near a wall have been reviewed by Bushnell (1983), Bandyopadhyay (1986, 1990) and Gad-el-Hak (1989). Investigations suggest that there is a greater potential for turbulence quieting and drag reduction in turbulent boundary layers than was realized previously. The experiments of Bechert (Bruse et al. 1993) show that it is now possible to achieve a net drag reduction of 10 percent with new hybrid surfaces, which is higher than the maximum achieved by any riblet (8 percent). On the other hand, numerically, Jung et al. (1992) have shown that a spanwise oscillation can lead to 40 percent reduction in near-wall vorticity fluctuations and drag. The entire surface is subjected to the perturbation, and the appealing feature is that no phase-tracking of the constituent hairpin vortices is required. The closed-loop control and dynamical systems methodology of Keefe (1993) shows that a drag reduction of 20 to 40 percent may be achievable. Finally, Handler et al. (1993) have shown that forcing at certain large length scales can lead to a drag reduction of 58 percent. However, because these studies are based on low Reynolds number channel simulations, the potential should be treated with caution (Bandyopadhyay and Gad-el-Hak 1993). Furthermore, implementing these strategies always involves a great deal of penalty and many technological challenges. In any case, clearly, the subject is receiving a great deal of attention, and new efforts are needed to bridge the wide gap that exists between the results attained in numerical simulations and experiments.

The methodology for the control of turbulence in a boundary layer that the present approach relies on, is called "selective suction and injection." The experiments of Gad-el-Hak and Blackwelder (1989) in a synthetic low Reynolds number boundary layer show that, a suction, when applied in phase to a convecting hairpin vortex, can reduce drag up to 60 percent and suppress turbulence spikes almost completely. The suction required is 1/5th of that when it is applied continuously. The low Reynolds number channel flow simulations of Moin et al. (1989) show that a selective suction-injection cycle applied in phase with the passage of hairpin vortices can suppress turbulence throughout the boundary layer and reduce drag by 25 to 30 percent.

The concept of turbulence control employed in this work is depicted in figure 1, which shows the vortex flow model, the wall-pressure signature (p_W) when there is no control, and the selective suctions and injections (q) applied for control (Bandyopadhyay and Balasubramanian 1993 a and b). Consider two hairpin vortices spaced apart in the streamwise direction. They produce positive pressure pulses on the wall and the induced motion between the legs of the hairpin vortices is of the ejection type. On the other hand, in the region between the two hairpin vortices, there is a sweep motion, and it produces a negative pressure pulse (Johansson et al. 1987). Suction and injection, which are phase-matched to the passage of the hairpin vortices, are applied in the specific areas, as shown in figure 1, to cancel the positive and negative pressure pulses. The elastic microfabricated surface (EMFS) elements being developed (figures 2 through 6) are expected to carry out these suctions and injections. The application of this control concept is described in greater detail in section 3.

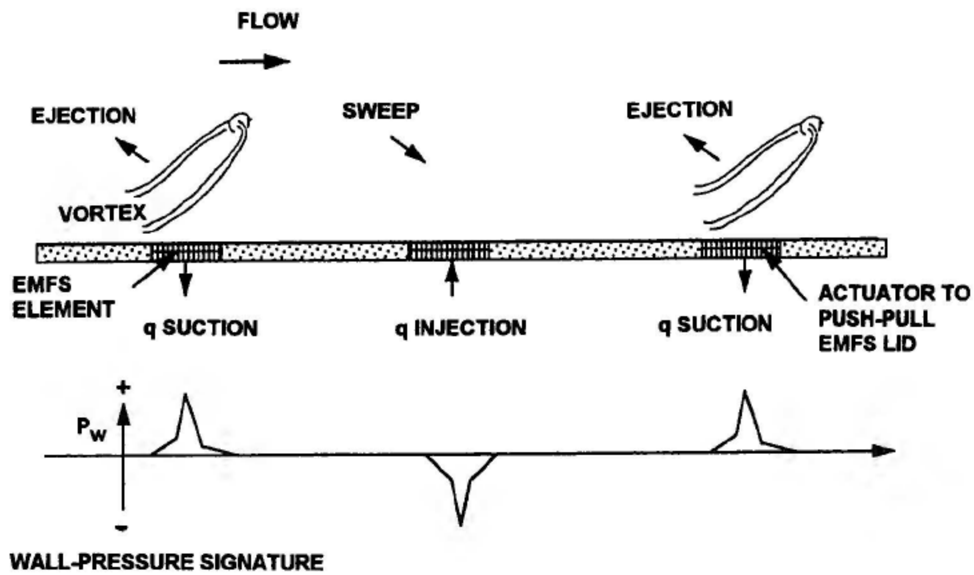

Figure 1. Sketch of the Flow Model and the Control Concept

2. OBJECTIVES

Experiments and low Reynolds number computer simulations have shown that the production of turbulence in a turbulent boundary layer is an intermittent (quasi-periodic) and a highly localized process. A high-amplitude (three-dimensional), traveling, wall-pressure pulse is associated with this (Johansson et al. 1987). The long-term purpose of this research is to develop an "active wall" with imbedded sensors and actuators that can react to this pressure-pulse, and then attenuate the production of turbulence. The short-term goal was to microfabricate an elastic surface for applications in high Reynolds number flows that can passively respond to the passing pressure pulse and then apply a suitable suction and injection.

3. APPROACH AND PROGRESS

At momentum thickness Reynolds numbers greater than 20 x 10^3 say, the length scales of the near-wall bursting cycle in water are about 3 mm and 0.2 mm in the streamwise and spanwise directions, respectively, and the time scales are about 1 ms (see quantities marked with an * in table 1) (Bandyopadhyay and Balasubramanian 1993a and b; Bandyopadhyay and Gad-el-Hak 1993). A surface that can respond to turbulence at these scales, can be produced by the so called technology of microfabrication, also known as MEMS (micro-electro-mechanical systems) (Bandyopadhyay 1993a, b, and c). Here, the integrated circuit silicon technology is being applied to mechanical engineering. The crystalline perfection of a single crystal silicon gives dimensional precision at micron levels, and its amenability to batch processing leads to affordability. These and other characteristics have led to an interest in the applications of this emerging technology to fluid mechanics.

Table 1. Typical Specifications of the Turbulent Boundary Layer

Nomenclature [a]	Units	NLON Quiet Water Tunnel [b]	Submarine [c]	Torpedo [d] (BTV Cruise)
Re_θ	--	$2.17x10^4$	$0.7x10^6$	$8.06x10^4$
U_∞	m/s	6.1	15	24.5
δ	mm	31	500	41
U_τ	m/s	0.21	0.3	0.62
ν	m^2/s $(x10^{-6})$	1	1	0.95
f_b*	Hz	40	6	12
λ_x^+	mm	2.3	2	0.75
λ_z^+	mm	0.46	0.4	0.15
$10\,\nu/U\tau$ (ten wall units)	mm	0.046	0.04	0.015
Δx_b*	mm	2.9	3.5	1.3
Δz_b*	mm	0.23	0.2	0.075
A*	--	1.6	1.14	1.15
$U_\tau\delta/\nu$	--	$6.5x10^3$	$150x10^3$	$2.7x10^3$
p_{rms}^2/τ_ω^2	--	12	14 - 18	10
Time Constant * $100\,\nu/U_\tau^2$	ms	2.3	1.1	0.3

(a) Nomenclature is defined as follows: $Re_\theta = U_\infty\theta/\nu$, where U_∞ is the freestream velocity, θ is the momentum thickness, and ν is the kinematic viscosity of the fluid; δ is the boundary layer thickness; U_τ is the friction velocity; f_b is the burst frequency, assuming an outer

layer scaling; λ_x^+ and λ_z^+ are the estimated streamwise (500 wall units) and spanwise (100 wall units) spacings of bursts; Δx_b, Δz_b are the estimated streamwise and spanwise lengths of the burst imprint; A is the burst area density, $(\lambda_x^+ \lambda_z^+)/(\Delta x_b \Delta z_b)$; $U_\tau\delta/\nu$ is a Reynolds number denoting the thinning of the viscous sublayer with respect to the outer layer with increasing Re_θ; p_{rms} is the root mean square of the wall-pressure fluctuations and τ_ω is the wall-shear stress. (b) The water tunnel data are from measurements by Keith & Bennet (1991) at the Naval Undersea Warfare Center Detachment, New London, CT (NLON). (c) The submarine data are estimated from a 1/7th power law velocity profile at the midpoint of a 180-m-long vehicle (Wilkinson 1990). (d) The torpedo data from Philips (1992) are from the midpoint of a 6-m-long high-speed buoyant test vehicle (BTV) and are calculated using the TAPS computer code.

3.1 FABRICATION OF ELASTIC MICROFABRICATED SURFACES (EMFS)

The layout of the microfabricated surface is shown in figures 2 and 3. Figure 4 is a scanning electron microscope photograph of the top-surface showing the staggered elements. Figure 5 shows the dimensions of the surface achieved after fabrication. A 10-inch-diameter stainless steel test plug was machined for water tunnel tests, which contained the openings for a plug containing the EMFS, and a sensor plug situated downstream. Several 3-inch-diameter brass plugs (figure 6) have been constructed to safely house and handle the silicon wafers, and they also fit inside the 10-inch-diameter plug. This smaller plug contains appropriate plumbing into which the epoxy can be poured to hold the wafer to the plug. A process has been developed to epoxy the wafer to the plug, both to ensure a flush fitting with the tunnel wall, and to make the wafer secure when the plug is being handled.

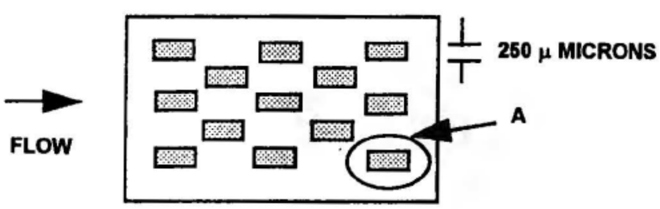

Figure 2. Top View of the Surface

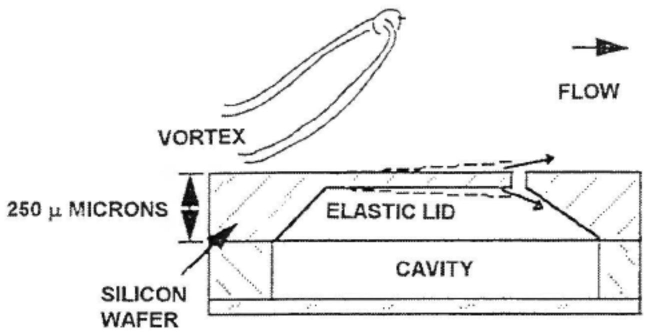

Figure 3. Sectional Side View of the Area Marked A in Figure 2

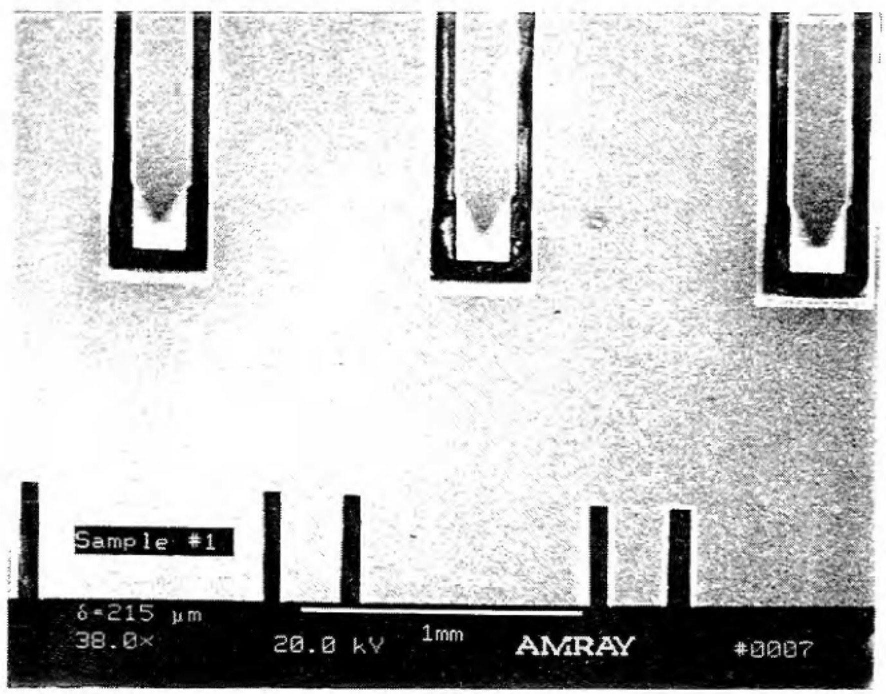

Figure 4. Scanning-Electron-Microscopic View of the Microfabricated Surface Elements (Flow direction is downward)

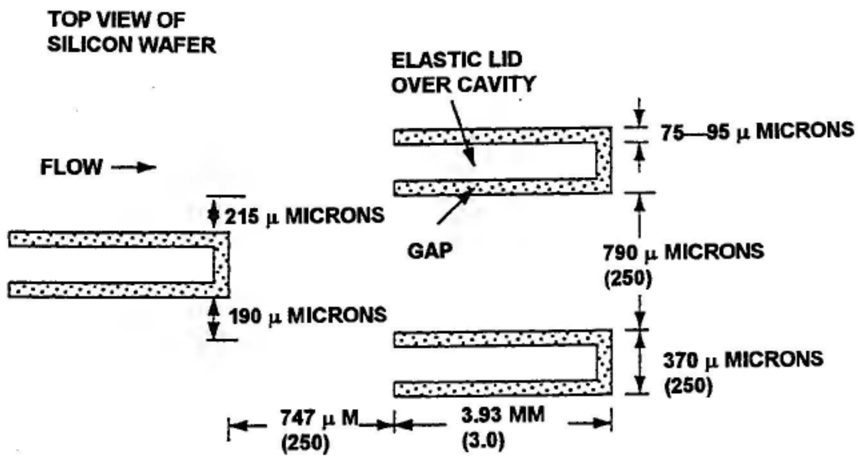

(SPECIFICATIONS BEFORE FABRICATION ARE IN PARENTHESES)

Figure 5. Dimensions of the Surface-Top After Microfabrication

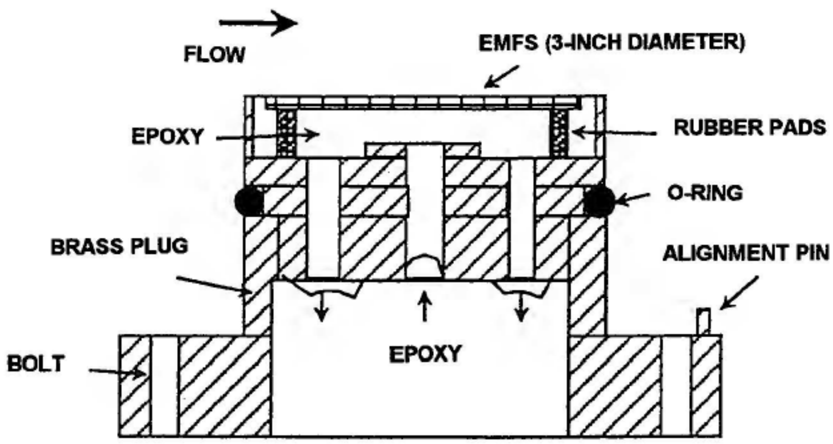

Figure 6. A Water Tunnel Test Plug Containing the EMFS

Earlier, plugs were constructed to practice the handling of the epoxy and its curing. These basic procedures are now used routinely and allows safe handling and testing of the wafers in a water or wind tunnel. Figure 7 shows a photograph of the water tunnel test plug with the EMFS wafer installed.

Four 3-inch-diameter single-crystal silicon wafers have been microfabricated at a cost of \$2.2K. Further copies of the die can be made at a lower cost. Each 3-inch-diameter piece actually consists of two wafers epoxied one above the other. The top wafer (figure 2) contains the appropriately spaced (figures 3 and 5) cavity openings covered with flexible lids, while the bottom wafer has partitioned rows of etched trenches, which run along the spanwise arrays of the cavities. In a preliminary passive concept of the design, the individual surface elements are interconnected along the span by means of these trenches, which facilitate venting for wall-pressure equalization and damping. The significance of the successful fabrication is that this is a first crucial step in the application of microfabrication to turbulence control at high Reynolds numbers. It demonstrates that surfaces that attempt to monitor the minute individual spatial scales of turbulence-production, which are typical of a high Reynolds number flow (table 1), can indeed be constructed. Future work to develop an active version of the surface, containing sensors and actuators, will be based on this basic EMFS.

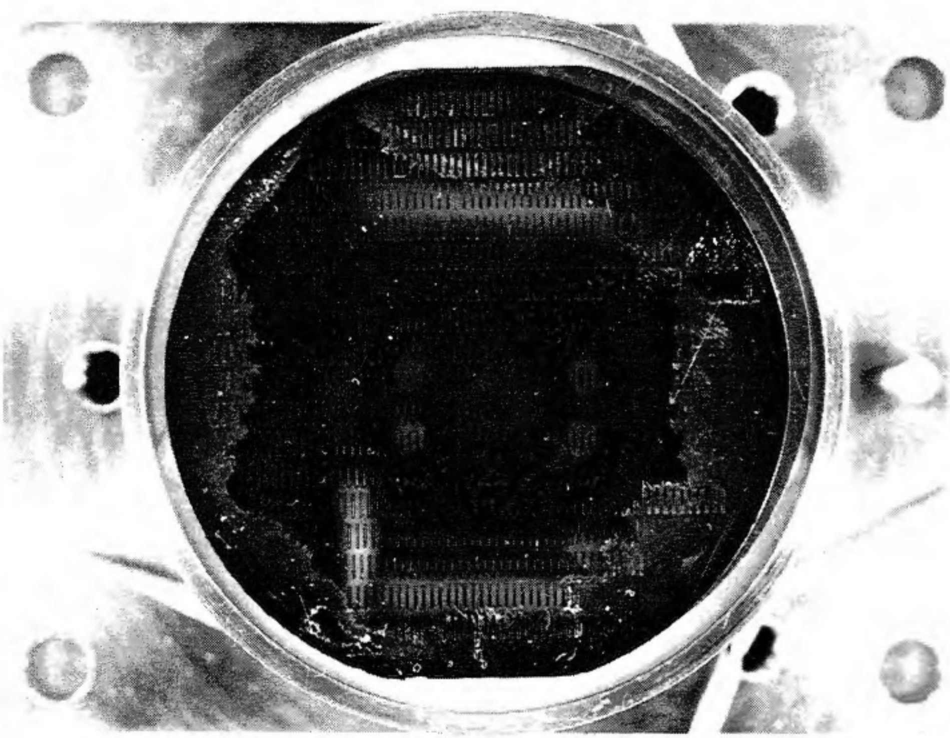

Figure 7. Photograph of the Water Tunnel Test Plug

3.2 HYDRO-ELASTIC PROPERTIES OF EMFS LIDS

The hydro-elastic properties of the EMFS lids were tested to measure the pressure difference between the top and bottom surfaces of the lid of the elastic EMFS element that is required to produce a certain deflection of the lid. This information will be used as follows:

(1) To determine the appropriate thickness of the lid, and its elastic properties, so that the lid could respond to a variable speed;

(2) To determine the loads that a future actuator has to move, and

(3) To validate hydro-elastic calculations of the concept, particularly the phase of the lid deflection versus the convection of a vortex.

A small manifold was constructed to fit under a row of cavities. The small deflection of the lid (microns) was measured by triangulation with a long reflecting laser beam (2.3 m). Figure 8 shows the deflection variation of the tip of the lid caused by the load of a fluid injection applied through it and expressed by the pressure differential across the top and bottom surfaces of the lid.

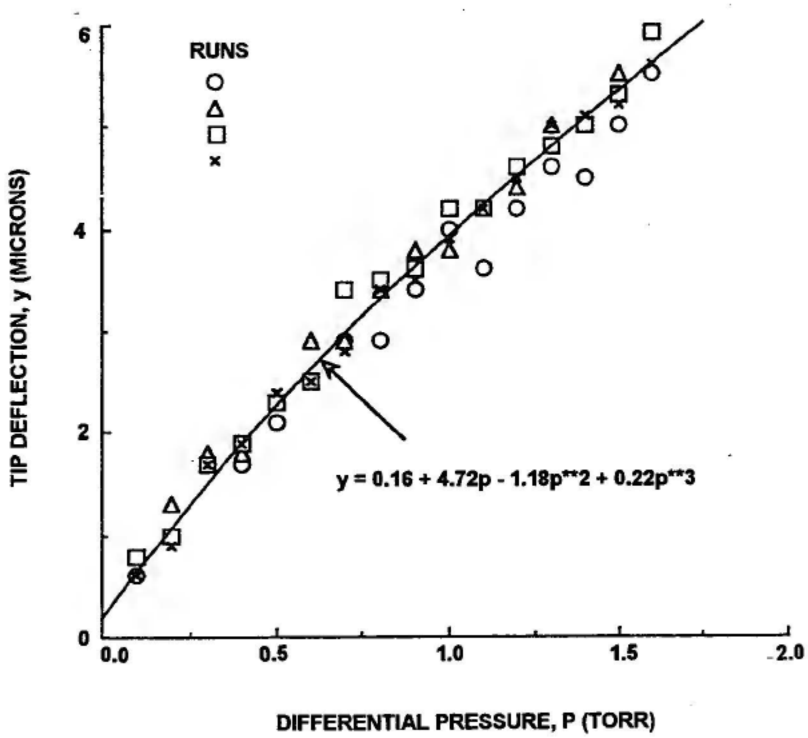

Figure 8. Elastic Lid Deflection Characteristics Under a Pressure Differential Loading

3.3 WATER TUNNEL TESTS

A hydrophone was placed at about 2.3 inches downstream (~2.5 δ) from the trailing end of the control surface (EMFS). The measured wall-pressure spectra are compared in figure 9 with the baseline smooth flat plate measurements. In each spectra shown in figure 9, 500 individual spectrum have been averaged. The control surface has not created any undesirable amplification of turbulence energy similar to those in rough walls.

In figure 9 the sensor is ~ 2.5δ downstream of the control surface. This is too great a distance for any near-wall control effect to last. For this reason, further tests have been conducted with a sensor placed much closer (~ 0.5 inch). These results are shown in figure 10. Again, each spectrum in figure 10 is an average of 500 individual spectrum. Figure 10 shows that the EMFS has not interacted with the boundary layer turbulence in a significant manner. However, figure 10 weakly suggests that the EMFS wall-pressure spectrum may be marginally lower than that in the smooth wall case at low Reynolds numbers, gradually becoming higher at higher Reynolds numbers. This trend will be verified in tests with future EMFSs. Laser Doppler velocimetry measurements of streamwise turbulence will also be carried out right over the EMFS.

The control surface (EMFS) in figures 9 and 10 had lids that were 50 μm thick. New surfaces are being fabricated with a lid thickness of 10 μm. Because deflection is proportional to the cube of the thickness, it is hoped that the lids will react to the turbulence better in the surfaces with thinner lids.

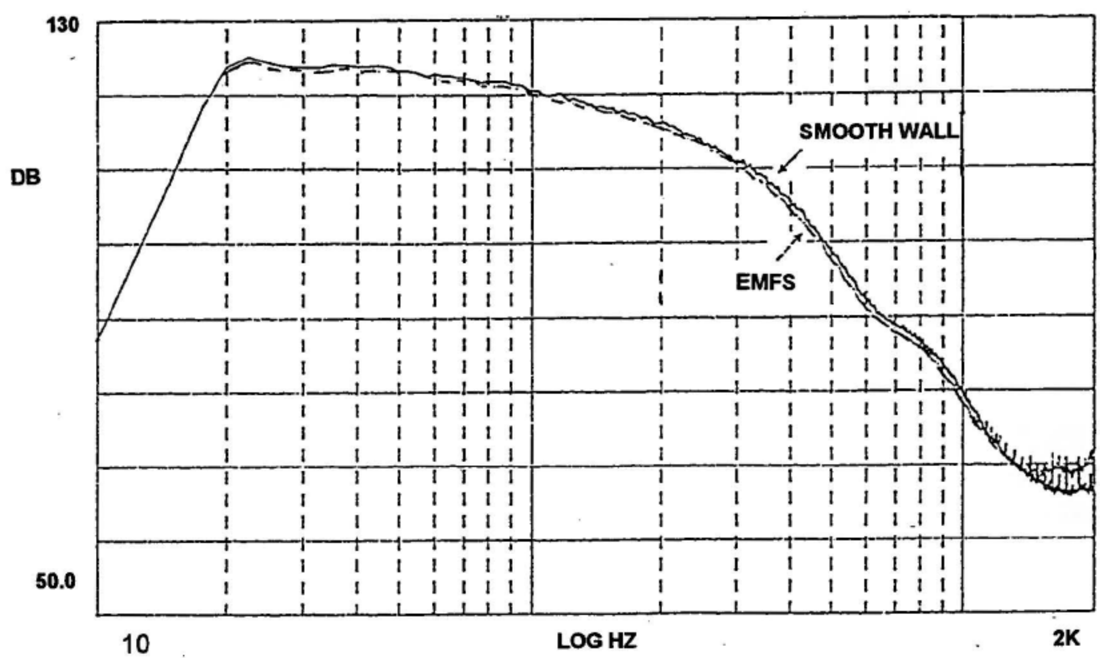

Figure 9. Comparison of Wall-Pressure Spectra ~2.5δ Downstream of the EMFS in the Water Tunnel ($U_\infty = 9.2$ ft/sec, $\mathrm{Re}_\theta = 20\times10^3$)

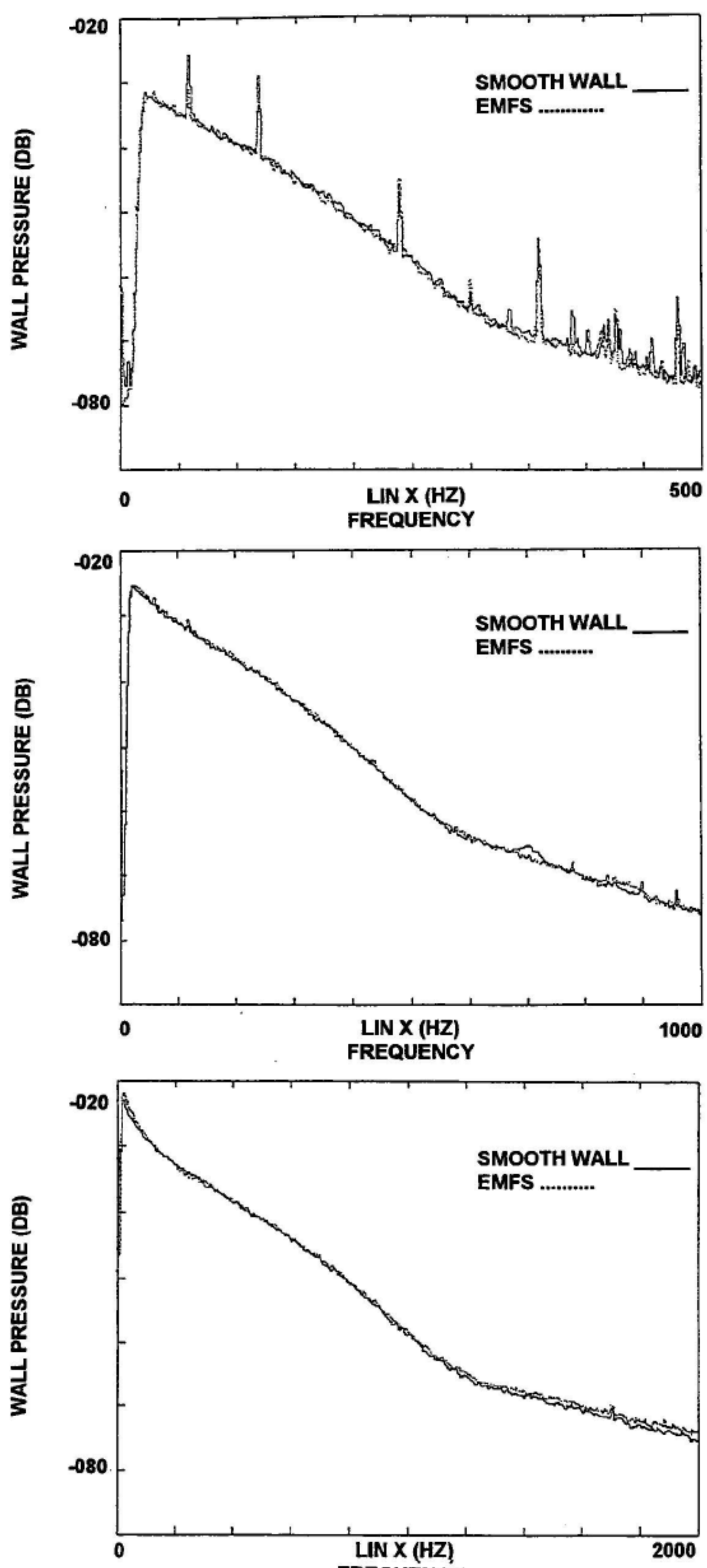

Figure 10. Comparison of Wall Pressure Spectra 0.54δ Downstream of the EMFS in the Water Tunnel (Top—Freestream Speed 4.6 ft/sec; Middle—9.3 ft/sec; Bottom—20 ft/sec)

4. FUTURE WORK

Figure 11 shows a schematic of the integrated sensor, EMFS, and actuator. In an active control design, it is estimated that the sensor power consumption is about 1 percent of the total drag, and the actuator power consumption is about 4 percent. They add up to a total drag penalty of 5 percent. Theoretically, the scheme can then offer a net drag reduction of 15 to 35 percent in a turbulent boundary layer, and a wall-pressure fluctuation reduction of about 5 dB. Future work will be conducted in several stages. In FY 1994, a cluster of shear sensors (hot-film or floating-element drag balance) will be microfabricated and tested in water. A recent development in microfabricated sensors for turbulence measurements is given by Löfdahl et al. (1992), and the level of effort required for the development of a cluster of such sensors can be gleaned from that article. The lid actuation and the development of a closed-loop control system will be undertaken in FY 1995.

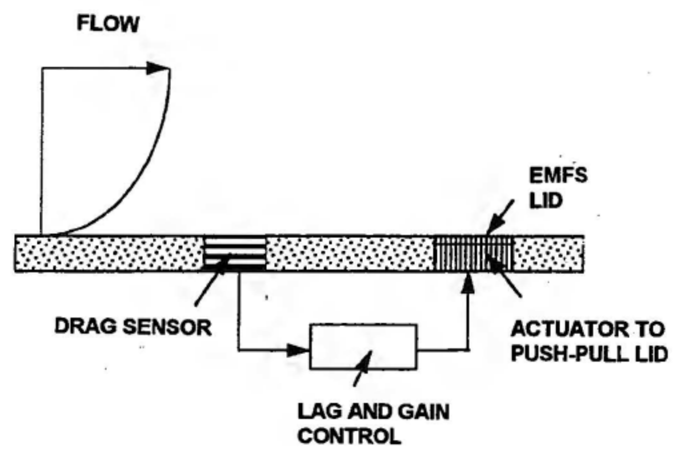

Figure 11. Schematic of the Integrated Drag Sensor, EMFS, and Actuator

5. CONCLUSIONS

The hydrodynamic tests show that the control surfaces did not behave as a roughness and did not show any adverse behavior. The engineering progress is noteworthy. After testing an EMFS in the water tunnel for 10 hours, one finds no degradation such as breaking of the cantilever lids, watermarks, or permanent deformations. The surface plugs are easy to handle, install, and remove from the water tunnel. Tests have been run at up to 40 psi without any damage to the wafers. The tests are repeatable to standard experimental uncertainties. It is expected that the wafer plugs will survive the BTV popup tests.

The present approach to turbulence control is more scientific than the notions of compliant walls, and physical spacings of the surface elements correlate with those of the turbulence structures. Individual cantilever lid stiffness is measurable, while in the compliant walls, at best, the bulk modulus is measured.

The fundamental engineering feasibility of the design and its working in the water tunnel have been demonstrated. The surfaces do not exhibit any roughness-like hydrodynamic behavior. The work in this study is the next logical step from riblets and compliant walls, which are two well-known methods of turbulence control.

6. BIBLIOGRAPHY

Bandyopadhyay, P. R.(1986), "REVIEW - Mean Flow in Turbulent Boundary Layers Disturbed to Alter Skin Friction," *ASME Transactions of the Journal of Fluids Engineering,* vol. 108, pp. 127-40.

Bandyopadhyay, P. R. (1990), "Convex Curvature Concept of Viscous Drag Reduction," in *Viscous Drag Reduction in Boundary Layers, Progress in Aeronautics and Astronautics Series,* vol. 123, pp. 285-324.

Bandyopadhyay, P. R. (Compiler) (1993a), *"Proceedings of the NUWC Division Newport Seminar Series on Microfabrication and Turbulence,"* NUWC-NPT TM 932089, Naval Undersea Warfare Center Division, Newport, RI.

Bandyopadhyay, P. R. (1993b), "Elastic Microfabricated Surface for Reducing Turbulence and Drag on an Object While it Moves Through a Fluid Medium," Navy Case Number 75126, Patent Application Serial Number 08/069, 820.

Bandyopadhyay, P. R. (1993c), "Micron-Sized Floating Element Drag Sensor for Shear Stress Measurements Away From Wall," Navy Case Number 75305.

Bandyopadhyay, P. R. and R. Balasubramanian (1993a), "Vortex Reynolds Number in Turbulent Boundary Layers," *Journal of Theoretical and Computational Fluid Dynamics* (Due to appear).

Bandyopadhyay, P. R. and R. Balasubramanian (1993b), "A Vortex Model for Calculating Wall Pressure Fluctuations," ASME *Symposium on Flow Noise Modeling, Measurement, and Control,* 28 November-3 December 1993, New Orleans, LA, NCA vol. 15, FED vol. 168, pp. 13-24.

Bandyopadhyay, P. R. and M. Gad-el-Hak (1993), "Reynolds Number Effects in Wall Bounded Turbulent Flows," NUWC-NPT Technical Report 10,296, Naval Undersea Warfare Center, Newport, RI (In production).

Bruse, M., D. W. Bechert, J. G.Th. van der Hoeven, W. Hage, and G. Hoppe (1993), "Experiments with Conventional and with Novel Adjustable Drag-Reducing Surfaces," in *Near-Wall Turbulent Flows,* R. M. C. So, C. G. Speziale, and B. E. Launder, eds., Elsevier Publishing, NY, pp. 719-738.

Bushnell, D. M. (1983), "Turbulent Drag Reduction for External Flows," *AIAA Paper No. 83-0227.*

Gad-el-Hak, M. (1989), "Flow Control," *ASME Applied Mechanics Review,* vol. 9, pp. 447-468.

Gad-el-Hak, M. and R. F. Blackwelder (1989), "Selective Suction for Controlling Bursting Events in a Boundary Layer," *AIAA Journal,* vol. 27, pp. 308-314.

Handler, R. A., E. Levich, and L. Sirovich (1993), "Drag-Reduction in Turbulent Channel Flow by Phase Randomization," *Physics of Fluids A*, vol. 5(3), pp. 686-694.

Johansson, A. V., J. Her, and J. H. Haritonidis (1987), "On the Generation of High-Amplitude Wall-Pressure Peaks in Turbulent Boundary Layers and Spots," *Journal of Fluid Mechanics,* vol. 175, pp. 119-142.

Jung, W. J., N. Mangiavacchi, and R. Akhavan (1992), "Suppression of Turbulence in Wall-Bounded Flows by High-Frequency Spanwise Oscillations," *Physics of Fluids A,* vol. 4, no. 8, pp. 1605-1607.

Keefe, L. R. (1993), "Drag Reduction in Channel Flow Using Nonlinear Control," AIAA *Paper No. AIAA 93-3279.*

Keith, W. L. and J. C. Bennett (1991), "Hydroacoustic Research at the Quiet Water Tunnel Facility of the Naval Underwater Systems Center," NUSC Reprint Report 8999, Naval Underwater Systems Center; New London, CT.

Löfdahl, L., G. Stemme, and B. Johansson (1992), "Silicon Based Flow Sensors Used for Mean Velocity and Turbulence Measurements," *Experiments in Fluids*, vol. 12, pp. 270-276.

Moin, P., J. Kim, and H. Choi, (1989), "On the Active Control of Wall-Bounded Turbulent Flows," Paper No. *AIAA-89-0960.*

Private Communication with R. B. Philips (1992), Naval Undersea Warfare Center Division, Newport, RI.

Wilkinson, S. P. (1990), "Interactive Wall Turbulence Control," in *Viscous Drag Reduction in Boundary Layers, Progress in Astronautics and Aeronautics Series,* vol. 123, pp. 479-509.

INITIAL DISTRIBUTION LIST

Addressee	No. of Copies
Center for Naval Analyses	2
Defense Technical Information Center	12